RSC Advances

ROYAL SOCIETY OF CHEMISTRY

www.rsc.org/advances

Effect of dopant concentration on the spectroscopic properties in In^{3+} doped (0,1,2 and 4 mol%) Yb: Tm: $LiNbO_3$ crystal

Li Dai [a, b *], Zhehua Yan [a], Shanshan Jiao [a], Chao Xu [b], Yuheng Xu [b]

a. Applied Science College, Harbin University of Science and Technology, Harbin 150080, China;
b. State Key laboratory of Crystal Material, Shandong University, Jinan ,250100, China
c. Department of the applied chemistry, Harbin Institute of Technology, Harbin 150001, China;

Abstract

A series of Yb: Tm: $LiNbO_3$ crystals with x mol% In^{3+} ions (x=0, 1,2 and 4 mol %) were grown by conventional Czochralski technique at the first time. The In , Yb and Tm contents in the crystals were measured by an inductively coupled plasma atomic emission spectrometer (ICP-AES). The results revealed that the segregation coefficients of Yb^{3+} and Tm^{3+} ions decreased with increasing of the In^{3+} doping concentration. Also the segregation coefficient of In^{3+} ion increases with the increasing In^{3+} doping concentration in the melts, and it is close to one. The IR transmission spectra and UV-Vis spectra were measured to analyze the defect structure of the crystals.

Keyword：In: Yb: Tm: $LiNbO_3$,crystal growth, dopant concentration, spectroscopic properties

1. Introduction

Tm^{3+}-based lasers emitting in the wavelength region of 2 μm have attracted much attention in recent years such as in atmospheric, telecommunications medicinal, and space applications fields [1-3]. The line width of Tm^{3+} ions (associated with $^3F_4 \rightarrow {}^3H_6$ transitions) corresponds to the wavelength range of 2 μm, which is similar to the Ho^{3+} ions(associated with $^5I_7 \rightarrow {}^5I_8$ transitions) , but the absorption range is wide and the absorption cross section is large. $LiNbO_3$ crystal is an excellent material exhibiting

* Corresponding author.Tel:+86 451 86390731.
E-mail address : daili198108@126.com(L.Dai)

desirable characteristics such as electro-optic, acousto-optic, piezo-electric and nonlinear optical performances [4, 5]. From a materials point of view, several RE-doped $LiNbO_3$ have been under study in the form of solid state laser devices and planar waveguide lasers. Yb^{3+} ion co-doped crystals have received considerable attention due to its high absorption cross-section in the near- infrared, suitable for convenient excitation with commercially available optical sources. Recently, many efforts have been devoted to the upconversion luminescence property in RE-doped $LiNbO_3$ crystal. The basic optical properties of Tm: $LiNbO_3$ and Yb: $LiNbO_3$ crystals have been already investigated [6,7] and are considered to be excellent upconversion media. Unfortunately, to our best knowledge, the properties of Yb:Tm: $LiNbO_3$ crystal is still to be scrutinized. In recent years, 2 μm lasers have attracted a large amount of interests due to their wide tenability and high efficiency ,which have increasingly important application in remote sensing, lidar and material processing , etc. It is believed that the study of Yb:Tm: $LiNbO_3$ crystals will be attractive researches.

The light induced refractive index change, called photorefractive effect, limits the performance of Yb: Tm: $LiNbO_3$ crystals. Until now, the comprehensive studies on the suppression of the optical damage caused by the high laser intensity in $LiNbO_3$ crystal have been investigated. As an effective solution to this problem, it has been found that the significant resistance to optical damage in $LiNbO_3$ can be improved by doping with certain divalent , trivalent or tetravalent cations (such as Mg^{2+}, Zn^{2+}, In^{3+}, Sc^{3+}, Hf^{4+} and Zr^{4+}) above the threshold concentration, see Ref. [8-13].

In this Letter, In: Yb: Tm: $LiNbO_3$ crystals with different concentrations of In_2O_3 (0, 1, 2 and 4mol%) were successfully grown by the Czochralski method. The defect structures were analyzed via IR transmission spectrum and the UV-Vis absorption spectra. Finally, the mechanism of the relationship between the spectroscopic properties and the concentration of In_2O_3 was thoroughly discussed.

2. Experiments

In this experiment, congruent $LiNbO_3$ crystals codoped with 0.5 mol. %Yb_2O_3, 0.5 mol. % Tm_2O_3, and various concentration of In_2O_3 were grown. The composition of melt was chosen as Li/Nb = 48.6/51.4. The In_2O_3 concentrations were 0, 1, 2 and 4mol%, respectively, which were labeled as 1#, 2#, 3# and 4#, as are shown in table 1. All raw materials precisely weighed and thoroughly mixed for 24h, heated up to 750℃ for 2h to remove CO_2, and then further sintered at 1050℃ for 2h. The crystals were grown in open atmosphere by traditional Czochralski method along ferroelectric z-axis with the rotation rate of 15~20 r/min and pulling speed of 1~1.5mm/h. After growth, the crystals were cooled down to room temperature at a rate of 60 ℃/h. The crystals were polarized at 1200℃ with a current density of 5 mA/cm^2. The wafers with diameter of 10×20×2mm (x× z× y) were cut from the middle part along y-face and polished to optical grade both of sides for optical tests. Fig. 1 showed the wafers of four In:Yb:Tm:LiNbO3 samples in experiment.

Table 1

Composition of In: Yb: Tm: $LiNbO_3$ crystal and the size of crystal.

Sample	1#	2#	3#	4#
In^{3+} in the crystal (mol%)	-	0.762	1.654	3.956
K_{eff} of In^{3+}	-	0.762	0.827	0.989
Yb^{3+} in the crystal (mol%)	0.848	0.793	0.754	0.712
K_{eff} of Yb^{3+}	0.848	0.793	0.754	0.712
Tm^{3+} in the crystal (mol%)	0.877	0.849	0.831	0.816
K_{eff} of Tm^{3+}	0.877	0.849	0.831	0.816
Crystal size(mm^2)	Φ25×28	Φ25×38	Φ25×35	Φ25×25
Axial temperature gradient(ºC/cm)	25-30	30-45	30-35	30-35
Radial temperature gradient (ºC/cm)	4-6	4-6	3-5	3-5

We analyzed the concentration of In^{3+}, Yb^{3+} and Tm^{3+} in the crystals with an inductively coupled plasma atomic emission spectrometer (ICP-AES, Optima 5300DV). The X-ray powder diffraction patterns were recorded using a SHMADZU XRD-6000 diffractometer with monochromatic Cu Kα

radiation.The OH^- absorption spectra of In: Yb: Tm: $LiNbO_3$ crystals were recorded by an Avator-360 FT-IR spectrometer at room temperature. The scanning was carried out between 400 and 4000 cm^{-1} with the scanning step of 1 cm^{-1}. In our later discussion, 3400 to 3600 cm^{-1} was chosen as the effective range. The ultraviolet-visible (UV-Vis) absorption spectra of the samples were measured with a CARY UV-Visible spectrometer, with the incident light transmitting along the y axis at room temperature. The measurement range was from 300 to 1100 nm.

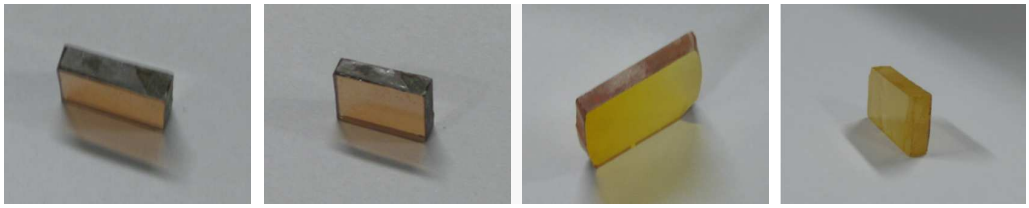

(a) 1# sample (b) 2# sample (c) 3# sample (d) 4# sample

Fig.1. Wafers of four In:Yb:Tm:$LiNbO_3$ crystals in experiment

3. Results and discussion

Preparation of standards solution: 99.99% purity In_2O_3 , Yb_2O_3 and Tm_2O_3 were put in Polytetrafluoroethylene (PTFE) beaker , plus nitric acid and hydrofluoric acid solution drops, and then dissolved by heating to make-up 40g / L stock solution and saved in PTFE bottle . From each top, middle and lower parts of the crystal, cut out a small crystal specimens and placed in an agate mortar grind into fine powder, with the balance millionth 0.05g powder sample is weighed out. Powder was placed in a PTFE beaker, added hydrofluoric acid and nitric acid solution each 5mL. After preheated for 25 minutes on a heated plate, using fully automated microwave digestion oven to microwave sample digestion. Then, the sample was heated and titrated with perchloric acid to eliminate hydrofluoric acid and protect the testing equipment from corrosion. At the same time, the digestive process was finished. After cooling to room temperature, the sample solution was mixed with 5% of

nitric acid and played in the 50 ml flask for testing, the volume of the solution was set up by addition of 5% of nitric acid. Fig. 1 showed the photos of the In:Yb:Tm:$LiNbO_3$ crystals samples.

The concentrations of In^{3+}, Yb^{3+} and Tm^{3+} ions in the In: Yb: Tm: $LiNbO_3$ crystals and effective distribution coefficient (K_{eff}) of ions are listed in Table 1. The effective distribution coefficient of In^{3+}, Yb^{3+} and Tm^{3+} ions are calculated by comparing the measured In^{3+}, Yb^{3+} and Tm^{3+} ions concentration in the crystal and melt. The dependence of the segregation coefficients of In^{3+}, Yb^{3+} and Tm^{3+} ions on the In_2O_3 concentration in the melts is shown in Fig. 2. It is clearly seen that the effective distribution coefficient of In^{3+} ion increases with the increasing In_2O_3 concentration in the melts, with the maximum close to one, indicating that it distributes uniformly in crystal. It can be further seen from Fig. 2 that the effective distribution coefficient of Yb^{3+} and Tm^{3+} ions decreases as the doping concentration of In^{3+} increases in the melts. When In^{3+} ion entered in Yb: Tm: $LiNbO_3$ crystal, it could readily occupy intrinsic defect (Nb_{Li}^{4+}) sites and the Nb_{Li}^{4+} concentration was sharply reduced, which suppressed the entrance of Yb^{3+} and Tm^{3+} ions into crystal. Thus，the effective distribution coefficient of ions Yb^{3+} and Tm^{3+} was continuously reduced.

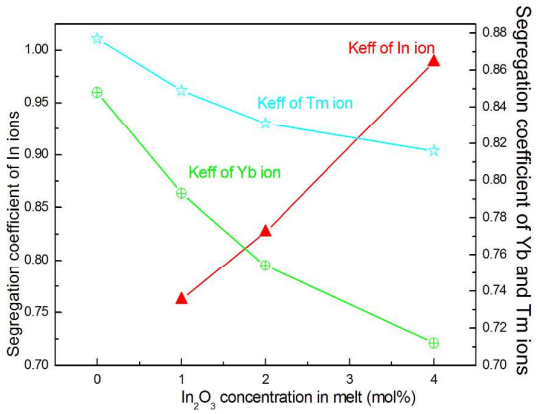

Fig. 2. The dependence of the segregation coefficient of In, Yb, and Tm ions on the In_2O_3 concentration in the melts.

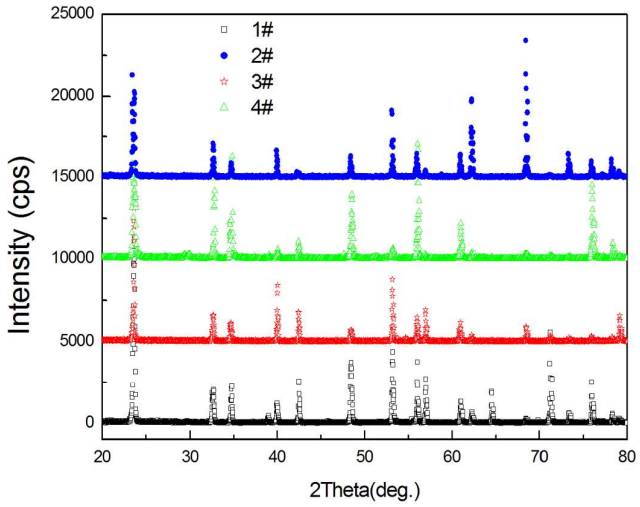

Fig. 3. X-ray powder diffraction patterns of In: Yb: Tm: $LiNbO_3$ crystals.

The XRD experimental results are shown in Fig 3. It can be seen that the dope of In^{3+}、Yb^{3+} and Tm^{3+} ions did not create new diffraction peak. This verified that after adding the In^{3+}、Yb^{3+} and Tm^{3+} ions to crystal lattice of $LiNbO_3$, the structure did not change dramatically [14]. Based on the ion radius approximation principle in the crystal field theory, the doped ion entered crystal lattice by replacing the Li^+ and Nb^{5+} ion instead of occupied the slot among crystal lattice. Hence to obtain the formulated In: Yb: Tm: $LiNbO_3$ crystals solid solution as a single phase.

In course of growth, H_2O vapors can be introduced into the crystals through formation of O-H bonds. The OH^- absorption spectra measurement results of In: Yb: Tm: $LiNbO_3$ crystals are represented in Fig. 4. Fig. 4 summarizes the OH^- absorption peak of samples 1#, 2# , 3# and 4# are located at 3482, 3482, 3507 and 3508 cm^{-1}, respectively. It can be found that the spectra belonging to In^{3+} of different concentration form different groups in In: Yb: Tm: $LiNbO_3$ crystals. According to Li-site vacancy model, in pure congruent $LiNbO_3$ crystal, the ratio of [Li]/[Nb] is 0.946. There always exist intrinsic

lattice defects, such as anti-site Nb (Nb_{Li}^{4+}) and Li vacancy (V_{Li}^{-})defects. The electropositive H^+ ions easily attracted by the electronegative V_{Li}^{-} and formed V_{Li}^{-}-OH^- complexes, whose vibrational absorption peak is located at 3482 cm^{-1} [15]. In Yb: Tm: $LiNbO_3$ crystals (i.e. for 1# sample), Yb^{3+} and Tm^{3+} replace Nb_{Li}^{4+}, forming Yb_{Li}^{2+} and Tm_{Li}^{2+}. When the concentration of In^{3+} ions is 1mol% in the melt, below its threshold value (i.e. for 2# sample) , Yb^{3+} and Tm^{3+} ions substitute for Nb_{Li}^{4+} defects and exist in the form of Yb_{Li}^{2+} and Tm_{Li}^{2+} in $LiNbO_3$, while these defects repel the H^+ and affect the V_{Li}^{-}-OH^- complexes only as ions around them and the peak position is at about 3482 cm^{-1}. When the concentration of In^{3+} ions exceeded the threshold (i.e. for 3# and 4# samples), all Nb_{Li}^{4+} defects disappear and In_{Nb}^{2-} defect structures appears as the In^{3+} ions enter the normal Nb sites. Meanwhile，the amount of Yb^{3+} and Tm^{3+} located at Nb sites increases, namely, the amount of Yb_{Nb}^{2-} and Tm_{Nb}^{2-} increases. The In_{Nb}^{2-} in the In_{Nb}-H-O defect structure has intensive attraction to H^+, more energy is required for O-H vibration, and the corresponding absorption is dominant at about 3507cm^{-1}. According to the analysis above，we can conclude that the In doping threshold concentration is about 1.5-2.0mol% as previously reported in [16-18].

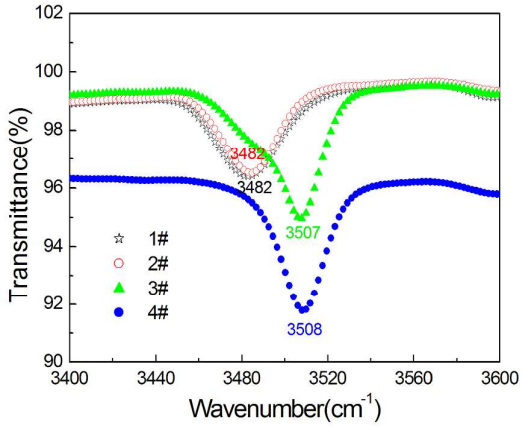

Fig.4. The IR absorption band related to the OH^- vibration in In:Yb:Tm:$LiNbO_3$ crystals

To confirm our significant conclusion, we further studied the UV-Visible absorption spectra of four

samples cut from the top, center and bottom of the grown crystals. Fig. 5 shows the UV-Visible absorption spectra of the In:Yb:Tm:$LiNbO_3$ crystals with different concentration of In^{3+}. The absorption edge of $LiNbO_3$ crystals is used to determine the composition [19]. The absorption edge at the level of a=15cm^{-1} or a=20 cm^{-1} is usually used to quantify the defects in a $LiNbO_3$ crystal [20]. In our experiment, the referred UV-Vis optical absorption coefficient for determination of the position defined as 20 cm^{-1}. It can be seen from Fig.5 that the UV-Vis absorption edges of the 1#， 2#，3# and 4# samples are located at 353, 346, 335 and 379 nm , respectively. The absorption peak of In: Yb: Tm: $LiNbO_3$ crystals is first violet-shifted with the increasing In_2O_3 doping concentration in the melt , then red-shifted when the doping concentration of In^{3+} is 4 mol%. The shift of absorption edge (4# sample) is up to 26 nm with respect to position of the Yb:Tm: $LiNbO_3$crystal. It is a remarkable fact that when In^{3+} doping concentration reaches 4.0 mol%, namely 4# sample，the absorption edge of shifts to the red substantially relative to 3#. There is some absorption band located at 300-1050nm, which is attributed to absorption of the $Tm^{3+}$and Yb^{3+}ions. The three absorption bands of Tm^{3+} ions centered at 465nm , 692 and 798nm are assigned to the $^3H_6 \rightarrow {}^1G_4$, $^3H_6 \rightarrow {}^3F_{2,3}$ and $^3H_6 \rightarrow {}^3H_4$ transitions [21]. And 980nm absorption peak correspond to transition from the $^2F_{7/2}$ ground state of Yb^{3+} ion to the excited state $^2F_{5/2}$.

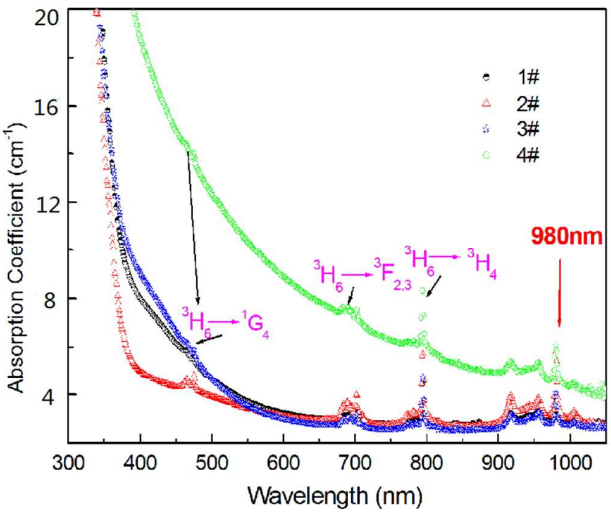

Fig.5. The UV-Vis absorption spectra of the In:Yb:Tm:$LiNbO_3$ crystals.

It's common knowledge that the shift of absorption edge can be explained by the polarization ability of the doped ions [22, 23]. The valence electron transition energy, which is from the 2p orbits of O^{2-} to the 4d orbits of Nb^{5+},determines the fundamental absorption edge of the $LiNbO_3$ crystal [23]. It can be concluded from the previous researches that the violet shift of the absorption edge is attributed to the increasing in the ability of adjacent dopant ions to polarize an O^{2-} ion shortens the band gap of the valence electron transition. Otherwise, the absorption edge of sample shifts toward the infrared band. In fact, the polarization ability of Nb^{5+} is smaller than that of In^{3+}, Yb^{3+} ,Tm^{3+} and Li^{+}. In Yb:Tm:$LiNbO_3$ crystal, Yb^{3+} ions and Tm^{3+} ions replace Nb_{Li}^{4+} and form Yb_{Li}^{2+} and Tm_{Li}^{2+}. When the In^{3+} enter Yb: Tm: $LiNbO_3$ crystals, because of the polarization ability of In^{3+} ions is much smaller than that of Nb_{Li}^{4+}, the absorption edge of In:Yb:Tm:$LiNbO_3$ crystal (2# sample) shifts to the ultraviolet band compared with that of Yb:Tm:$LiNbO_3$ crystal (1# sample) . When the concentration of In^{3+} ions in the melt exceeded the threshold value (3# sample), Nb_{Li}^{4+} defects almost disappeared, the In^{3+} ions began to enter the normal Li and a little bit of Nb sites. As the polarization ability of In^{3+} was lower than that of Li^{+}, which caused the deformation of O^{2-} ions electron clouds, the width of the forbidden band

increases and absorption edge continuous shifts to the violet. When the In_2O_3 doping concentration in the melts is up to 4.0mol% (4# sample) , part of In^{3+}, Yb^{3+} and Tm^{3+} ions begin occupies Nb sites form In_{Nb}^{2-}, Yb_{Nb}^{2-} and Tm_{Nb}^{2-}. As the polarization ability of In^{3+} ion is smaller than that of Nb^{5+}, red shift of the absorption edge in 4# relative to 1#. This discussion of dopant occupancy is consistent with the analysis result of experimental shown in OH^- absorption spectra.

4 .Conclusions

In conclusion, In: Yb: Tm: $LiNbO_3$ crystals with different concentrations of In_2O_3 (0, 1, 2 and 4 mol%) were successfully grown by the Czochralski method. The inductively coupled plasma optical emission spectrometry, IR transmission spectrum and the UV-Vis absorption spectra were measured and discussed in terms of the spectroscopic properties in In^{3+} doped (0, 1, 2 and 4 mol%) Yb: Tm: $LiNbO_3$ crystal. The effective distribution coefficient of In ion increases with the increasing In_2O_3 concentration in the melts, and it is close to one, indicating that In^{3+} distributes uniformly in crystal. The UV-Vis absorption spectra showed that the absorption edges of In:Yb:Tm: $LiNbO_3$ crystals is first violet-shifted with the increasing In_2O_3 doping concentration in the melt , then red-shifted when the doping concentration of In^{3+} is 4 mol%. It was suggested that for low concentration of In^{3+} ion, the all dopant ions first occupy the Nb anti-sites or Li vacancies and when the concentration of In^{3+} was reaches 4.0 mol% they may replace normal Nb sites.

Acknowledgments

This work is supported by National Natural Science Foundation of China (No. 51301055), Provincial University Key Lab Open Foundation for Materials Research and Application in Harbin University of Science and Technology (No.2013) and the Opening Project of State Key laboratory of Crystal Material (No.KF1409)

Reference

[1] A. Bensalah, K. Shimamura, V. Sudesh, et al., J. Cryst. Growth 223(2001) 539-544.

[2] R. A. McFarlane, Opt. Soc. Am. B 11(1994) 871-880.

[3] C. Li, X. Zhang, C. Wang, et al., Chin.J. Inorg. Chem. **27**(2011) 6-10.

[4] D. Janner, D. Tulli, M. García-Granda, M. Belmonte, V. Pruneri, Laser Photonics Rev. 3(2009)301-313.

[5] T. Y. Fan, A. Cordova-Plaza, M. J. F. Digonnet, R. L. Byer, H. J. Shaw, J. Opt. Soc. Am. B 3 (1986)140-148.

[6] M. Jelínek, J. Oswald, T. Kocourek, K. Rubešová, P. Nekvindová, D. Chvostová, A. Dejneka, V. Železný, V. Studnička and K.Jurek, Laser Phys. 23(2013)105819.

[7] V. T. Pham, S. K. Lee, M. T. Trinh, K. S. Lim, D. S. Hamilton, and K. Polgar, Opt. Commun., 248 (2005)89-96.

[8] T. R. Volk, N. M. Rubinina, Ferroelect. Lett 14(1992)37-43.

[9] X. Zhen, Q. Li, L. Wang, Y. Xu, J. Cryst. Growth 284(2005)270-274.

[10] S. Li, S. Liu, Y. Kong, J. Xu, G. Zhang, Appl. Phys. Lett 89(2006)101126-4.

[11] Z. Xu, Y. Xu, Mater Lett 61(2007) 3243-3246.

[12] L. Dai, Y. Su, S. Wu, J. Guo, C. Xu, Y. Xu.Opt. Commun 284(2011)1721-1725.

[13] L. Sun, F. Guo, Q. Lv, H. Yu, H. Li, W. Cai. Cryst. Res. Technol 42(2007)1117-1122.

[14] Fan Y, Cordova-Plaza A and Digonnet M J F.J. Opt. Soc. Am. B 3(1986) 140.

[15] O.F. Schirmer, O. Thiemann, M. Wöhlecke, J. Phys. Chem. Solids 52(1991)185-200.

[16] T. Volk, N. Rubinina, M. Wöhlecke, J. Opt. Soc. Am. B 11(1994)1681-1687.

[17] N.Y. Kamber, J. Xu, S.M. Mikha, G. Zhang, G. Zhang, Opt. Commun. 176 (2000) 91-96.

[18] H. Qiao, J. Xu, Q.Wu, X. Yu, Q. Sun, G. Zhang, X. Zhang, T. Volk, Opt. Mater. 23(2003) 269-277.

[19] I. Földvári, K. Polgár, R. Voszka, Crystal Research and Technology 19(1984) 1659-1661.

[20] K. Polgár, Á. Péter, L. Kovács, Journal of Crystal Growth 177(1997)211-216.

[21] C. Sun, F. Yang, T. Cao, Z. You, Y. Wang, J. Li, Z. Zhu, and C. Tu, J. Alloy Compd. 509 (2011) 6987-6993.

[22] L. Dai, C. Xu, Z. Qian, J. Li, D. Li, Y. Xu, J. Lumin 134(2013)255-259.

[23] W. Wang, X. Chen, D. Ni, D. Zhang, X. Wu, J. Alloys Compd. 402(2005)224-226.